

SAMPL9 blind predictions using nonequilibrium alchemical approaches

Piero Procacci^{1*} and Guido Guarnieri²

^{1*}Chemistry, University of Florence, Via Lastruccia 3, Sesto Fiorentino (FI), 50019, Italy.

²DTE-ITC, ENEA, Portici research center, P.le E. Fermi 1, Portici (NA), 80055, Italy.

*Corresponding author(s). E-mail(s): piero.procacci@unifi.it;
Contributing authors: guido.guarniri@enea.it;

Abstract

We present our blind predictions for the Statistical Assessment of the Modeling of Proteins and Ligands (SAMPL), 9th challenge, focusing on binding of WP6 (carboxy-pillar[6]arene) with ammonium/diammonium cationic guests. Host-guest binding free energies have been calculated using the recently developed virtual double system single box approach, based on the enhanced sampling of the bound and unbound end-states followed by fast switching nonequilibrium alchemical simulations [M Macchiagodena, M Pagliai, M Karrenbrock, G Guarnieri, F Iannone, Procacci, *J Chem Theory Comput*, 16, 7260, 2020]. As far as Pearson and Kendall coefficients are concerned, performances were acceptable and, in general, better than those we submitted for calixarenes, cucurbituril-like open cavitand, and beta-cyclodextrines in previous SAMPL host-guest challenges, confirming the reliability of nonequilibrium approaches for absolute binding free energy calculations. In comparison with previous submissions, we found nonetheless a rather large mean signed error that we attribute to the way the finite charge correction was addressed through the assumption of a neutralizing background plasma.

Keywords: SAMPL9, binding free energy, Non-equilibrium, Crooks theorem, fast switching, Hamiltonian Replica Exchange, HREX, Solute Tempering, WP6

1 Introduction

The Statistical Assessment of the Modeling of Proteins and Ligands (SAMPL) is a set of community-wide blind challenges aimed at advancing the computational techniques in drug design.[1–5]. New experimental data, such as dissociation free energies, hydration free energies, acid-base dissociation constants, or partition coefficients are withheld from participants until the prediction submission deadline, so that the true predictive power of methods can be assessed.

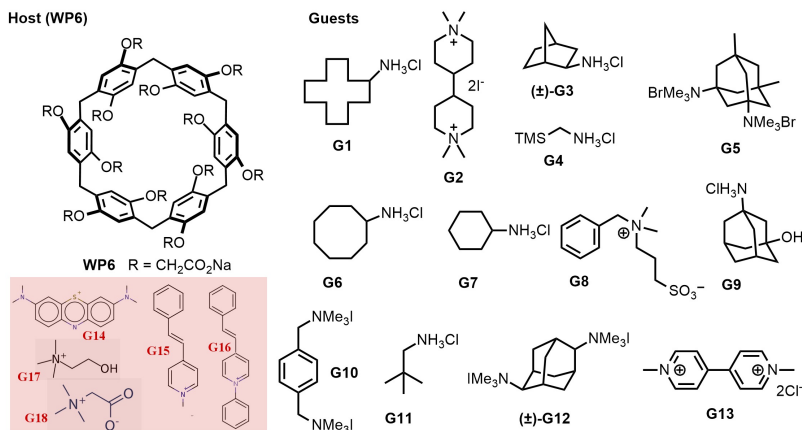


Fig. 1 Host-guest SAMPL9 challenge. In the shaded red area on the bottom left corner, the molecules with known binding affinities used for pre-assessment are reported (see text).

In the latest 9th challenge, participants were required to predict the binding affinities of thirteen ammonium/diammonium cationic ligands (guests) vs WP6, a water-soluble toroidal macrocyclic host molecule (see Figure 1). Host-guest experimental binding affinities, measured by Isothermal Titration Calorimetry (ICT) at pH=7.4 were disclosed by November 2021 and are now reported in Ref. [6]. Actually, the binding affinity of G13 (Paraquat) was available on literature at physiological pH[7, 8] *before* the submission deadline. The host WP6, never featured in previous SAMPL challenges, is structurally similar to cucurbit[n]urils (CBn) used in SAMPL6[3] and SAMPL8[9] with important differences related to the electrostatic interactions. Unlike the neutral CBn host, the quasi-D6h WP6 bears six carboxylated moieties on the upper and lower rims that can be in part protonated at pH=7.4.[7, 8] As the pK_a's of WP6 were not available, such a feature represented an important challenge in the blind prediction of WP6-guest binding affinities. Participants were in fact requested to deal with this complication.

In this report, we present the dissociation free energies of the fully anionic WP6⁻¹² for the thirteen cationic guests of Figure 1 plus five additional guest molecules with known dissociation constants, namely methylene blue (G14)[10], GNF-Pf-3194 (G15)[11], M2 (G16)[11], choline (G17)[12] and

betaine (G18)[12]. The calculations have been performed on the CRESCO6-ENEA cluster[13] in Portici (Italy) using the so-called virtual Double System Single Box (vDSSB) method[14–17], based on a production of a swarm of concurrent nonequilibrium (NE) alchemical simulations that are started from end-state canonical configurations sampled using Hamiltonian Replica Exchange (HREM)[18].

2 Methods

2.1 Estimation of the protonation state of WP6

As stated in the introduction, the twelve pKa’s of WP6 host were not known before the SAMPL9 deadline for submission. In presence of multiple host-guest complexes with various protonation states, the overall observed association constant for Gn-WP6 complexes is given by

$$K_a = \sum_k W_k K_a^{(k)} \quad (1)$$

where $K_a^{(k)}$ is the association constant for the k -th protonated WP6 species and W_k is the corresponding normalized weight. The Gn-WP6 dissociation free energy should be hence calculated as

$$\Delta G_d = RT \ln \sum_k W_k e^{\beta \Delta G_d^{(k)}} \quad (2)$$

where $\Delta G_d^{(k)}$ is the dissociation free energy with the host in the k -th protonation state. The predicted pKa of the WP6 template monobasic acid 2-(2,5-dimethylphenoxy) acetic acid is 3.23[19]. We assumed a pKa distribution modulated by the so-called statistical factor[20] for twelve equivalent protonation sites

$$\text{pKa}_n = \text{pKa}_1 - \log(n/13 - n) \quad (3)$$

where $\text{pKa}_1 = 3.23$ is that of the monobasic acid. We obtained that the prevalent species at $\text{pH}=7.4$ is the WP6^{-12} anion with all deprotonated carboxylated groups with a weight $W_{-12} = 0.98$, in surprisingly good agreement, despite the crudeness of our approach, with the experimental value of $W_{-12} = 0.95$ released after the submission deadline.[21]

We hence computed the dissociation constant for the WP6^{-12} species only, related to the chemical equilibrium



It should be nonetheless stressed that the large weight of the fully deprotonated species, $W=0.95$, does not guarantee that the experimental dissociation free energy corresponds to the dissociation free energy of the equilibrium Eq.

4. If the dissociation free energy of any of the other simultaneous chemical equilibria, $\text{WP6}^{-n}\text{Gn} \leftrightarrow \text{WP6}^{-n} + \text{Gn}$ with $n = 1\dots 11$, is much *larger* than that corresponding to the equilibrium Eq. 4, then, according to Eq. 2, the overall experimental free energy can be significantly higher than that matching the equilibrium Eq. 4. So our dissociation free energy, computed for the equilibrium 4, should be viewed as a *lower bound* for the true experimental dissociation free energy.

2.2 vDSSB approach for absolute dissociation free energies

The vDSSB methodology is thoroughly described in Ref. [15, 16]. In brief, the method consists of two massively parallel computational steps, the HREM stage and the nonequilibrium alchemical stage. The HREM stage relies on the enhanced sampling of the host-guest bound state (with the ligand at full coupling) in explicit water and of the isolated guest molecule. The initial configurations for the unbound state are prepared by combining the HREM-sampled gas-phase (decoupled) ligand snapshots with a pre-equilibrated box filled with explicit water. HREM uses $n = 16$ and $n = 8$ replicas for the bound and unbound states respectively, with a maximum scaling factor of $S = 0.1$ (corresponding to a temperature of 3000 K) involving only the intra-solute bonded and non-bonded interactions[22]. The scaling factors along the replica progression are computed according to the protocol $S_m = S^{(m-1)/n}$ with $m = 1\dots n$. Only the scaling factors are exchanged among neighboring replicas to minimize the communication overhead on the MPI layer. The HREM simulations are run for 48 ns and 16 ns for the bound and gas-phase state, respectively with exchange rates in the range 25%-50%.

In the NE alchemical stage, the bound state leg of the alchemical cycle is performed by rapidly decoupling the bound ligand in a swarm of 360 independent NE simulations, each lasting 1.44 ns. The unbound leg of the cycle is done by growing (recoupling) the ghost ligand in the solvent in 480 NE alchemical simulations lasting 0.36 ns. Electrostatic and Lennard-Jones interactions are switched off/on sequentially, in order to separate the corresponding contributions to the binding. For further details on the ligand coupling/decoupling protocols, we refer to Ref. [15, 16].

The final bound and unbound alchemical work distributions are combined in the convolution

$$P(W) = P_b * P_u(W) = \int dw P_b(W) P(W - w) dw \quad (5)$$

as if the two independent processes of the ligand annihilation in the bound state and of the ligand growth in the pure solvent occurred in the same box (hence the name vDSSB), with one ligand on the host and the other in the far distant bulk.

The dissociation free estimate can be performed by way of the Jarzynski identity[23]

$$\Delta G_{\text{vDSSB}} = -RT \ln \int P(W) e^{-\beta W} dW \quad (6)$$

or using the Crooks theorem[24] in the assumption that the convolution can be described by a mixture of normal distributions[15, 25], i.e

$$\Delta G_{\text{vDSSB}} = -RT \ln \sum_i c_i e^{-\beta(\mu_i - \frac{1}{2}\beta\sigma_i^2)} \quad (7)$$

where c_i , μ_i , σ_i^2 are the normalized weight, mean and variance of the i -th normal component, determined via the expectation-maximization algorithm [26, 27]. Estimates based on eq. 6 or eq. 7 are used depending on the width and character of the work distributions as assessed by the Anderson-Darling normality test [28]. The free energy estimates are corrected for a volume[29–31] and a charge term[30, 32] (for non-neutral ligand) given by

$$\Delta G_{\text{vol}} = RT \ln \left[4\pi \frac{(2\sigma)^3}{3V_0} \right] \quad (8)$$

$$\Delta G_{\text{fs}} = -\frac{\pi}{2\alpha^2} \left\{ \frac{[Q_H^2 - (Q_H + Q_G)^2]}{V_{\text{BOX}}^{(b)}} + \frac{Q_G^2}{V_{\text{BOX}}^{(u)}} \right\} \quad (9)$$

where σ is the standard deviation of the host-guest COM-COM distance distribution in the bound state, V_0 is the standard state volume, Q_G , Q_H are the net charges of the guest and the host, $V_{\text{BOX}}^{(b)}$, $V_{\text{BOX}}^{(u)}$ and are the mean volume of the MD box for the bound and unbound state respectively, and α is the Ewald convergence parameter. The effectiveness of the correction Eq. 9 for finite size effects when dealing with charged ligands has been amply assessed in [30], while the origin of the binding volume term Eq. 8 has been discussed in Refs. [29, 31, 33]. The final blind prediction for the standard dissociation free energy is given by

$$\Delta G_d^0 = \Delta G_{\text{vDSSB}} + \Delta G_{\text{vol}} + \Delta G_{\text{fs}} \quad (10)$$

2.3 Simulation setup and parameters

Guests and host PDB files were taken from the SAMPL9 GitHub site. For the two chiral compounds, the G3 guest (2-bicyclo[2.2.1]heptanyl]azanium) corresponds to the 1R 2R 4S diastereoisomer. The G12 guest (Hexamethyladamantane-2,6-diammonium) has the 2 and 6 carbon atoms of the R type. The Force Field (FF) parameters and topology of the host and guests molecules were prepared using the PrimaDORAC interface[34] based on the GAFF2[35] parameter set. For G4, the silicon-related parameters were taken from Ref. [36]. The initial bound state was prepared using the Autodock Vina code[37]. The bound complexes and the ghost ligands were solvated

in about 1600 and 512 OPC3[38] water molecules, respectively. Long-range electrostatic interactions were treated using the Smooth Particle Mesh Ewald method (SPME)[39]. A background neutralizing plasma was assumed within the SPME method[32]. The cut-off of the Lennard-Jones interactions was set to 13 Å. All simulations, HREM or nonequilibrium, were performed in the NPT ensemble in standard conditions using an isotropic Parrinello-Rahman Langrangian[40] and a series of Nosé thermostats[41] for pressure and temperature control, respectively. Bonds constraints were imposed on X-H bonds only, where X is a heavy atom. All other bonds were assumed to be flexible. In the bound state simulations (HREM or NE) the guest and the host center of mass (COM) were tethered by a weak harmonic potential with a force constant of $K = 0.06 \text{ kcal/mol } \text{Å}^{-2}$, corresponding to a ligand allowance volume of $\simeq 600 \text{ Å}^3$. All simulations have been done using the hybrid OpenMP-MPI program ORAC[42] on the CRESCO6 cluster[13].

3 Results

In Figure 3 we show the host-guest COM-COM distance distributions in the bound state for all thirteen SAMPL9 pairs as obtained from the target state HREM sampling of 48 ns. According to Eq. 8, the binding site volume is calculated from the variance of the COM-COM distribution as $V_{\text{site}} = 4\pi \frac{(2\sigma)^3}{3}$. As it can be seen, despite the weak tethering COM-COM harmonic potential and the correspondingly large allowance radius of $\simeq 8 \text{ Å}$ (exceeding substantially the radius of the WP6 cavity of $\simeq 5.4 \text{ Å}$), the guests never leave the WP6 pocket, with a standard deviation of the COM-COM distribution ranging from $\simeq 0.2 \text{ Å}$ (G7) to $\simeq 0.9 \text{ Å}$ (G10). As discussed in Ref. [31], the HREM approach with *intrasolute* (ligand and host) scaling does not accelerate passive diffusion with little impact on the k_{off} and on the ligand residence time (in the range of the microsecond to milliseconds for all ligands). On the Zenodo platform (<https://zenodo.org/record/5891191>) we provide the HREM-generated trajectories of the bound state for all thirteen guest-host systems.

In Table 1 we have collected all the quantities that have been used in the determination of the estimate of the standard dissociation free energy, Eq. 10, namely the charge and volume corrections (Eq. 8 and Eq. 9), the mean and variance of the bound and unbound work distributions as well as their character as assessed by the Anderson-Darling test. The bound and unbound work distributions, along with their convolution Eq. 5, are reported for all guests of Table 1 in the Electronic Supporting Information (ESI). The corresponding raw data of the work can be found on the Zenodo site (<https://zenodo.org/record/5891191>). The last column of Table 1 indicates the type of estimate for the alchemical dissociation free energies ΔG_{vDSSB} of the ranked submission: G_b refers to a Gaussian estimate, S_3 is an estimate based on the Gaussian mixture, Eq. 7, with three components, and finally the estimate $S_J + B$ is based on the Jarzynsky exponential average, Eq. 6.

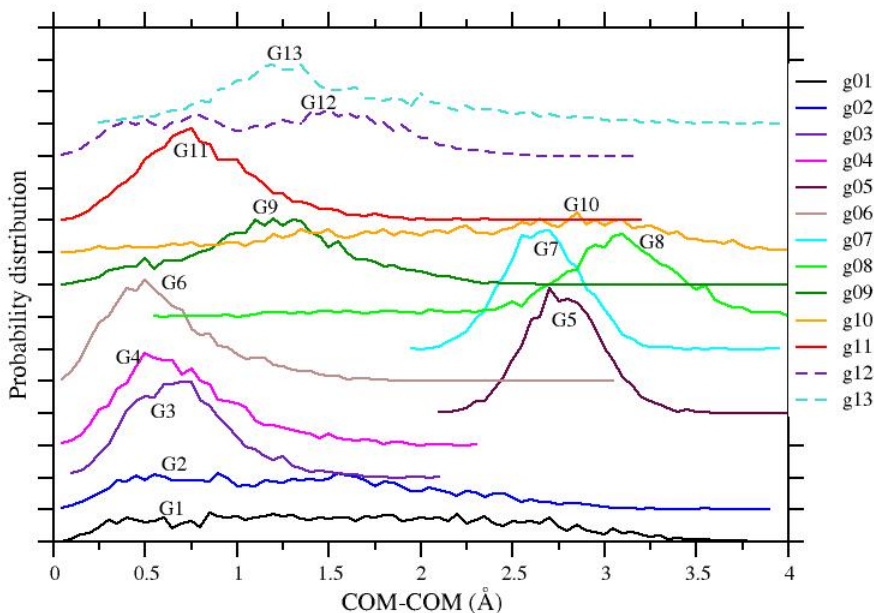


Fig. 2 Host-guest COM-COM distance distributions obtained from the HREM sampling of the bound state.

Ideally, such estimates should all converge to the same value when $n \rightarrow \infty$ and/or the duration of the NE process $\tau \rightarrow \infty$. For finite samples, their precision and accuracy are strongly affected by the spread (connected to the dissipation of the process[31]) and the character of the work distributions. The criteria for selecting the estimate type for each pair were the following: i) if both the bound and unbound work distributions prior to the convolution pass the Anderson-Darling test with a p-value[43] greater than 50% ($A^2 < 0.3$), then the Gaussian estimate is adopted; otherwise, ii) if the uncertainty is less than 2 kcal/mol we use S_3 ; otherwise iii) we use the Jarzynski estimate $S_J + B$, where to Eq. 6 is added a correction due to the bias. We recall that the *positive bias* bias in exponential averaging of the NE work is inescapable[44, 45]. The convolution, by boosting the sample size to $n = n_b \times n_u$, tames the bias but does not suppress it, notably when the width of the resulting distribution is large. As one can see from Table 1 and Figures S1-S18 of the ESI, in general, the width of the convolution is somewhat larger than the width of the *bound state* distribution, since $\sigma_u^2 < \sigma_b^2$, even if the duration time of the ligand annihilation in the bound state process (1.44 ns) is much longer than that of the ligand growth process in the bulk (0.36 ns). The variance of the convolution is in fact given by $\sigma_{BU}^2 \simeq \sigma_b^2 + \sigma_u^2$ (an equation that is *exact* if both distributions are

guest	ΔG_{vol}	ΔG_{fs}	$\langle W_b \rangle$	σ_b	$\langle W_u \rangle$	σ_u	AD _b	AD _u	σ_{BU}	Est. type
G1	-2.6	-2.0	75.9	3.2	-53.0	1.9	2.32	2.96	3.73	$S_J + B$
G2	-2.9	-4.3	147.6	2.3	-121.2	1.1	0.41	0.24	2.53	S_3
G3	-4.5	-2.0	78.5	2.8	-56.8	0.8	2.57	0.63	2.88	S_3
G4	-4.2	-2.0	73.8	2.2	-56.8	0.8	0.38	0.31	2.35	G_b
G5	-4.5	-4.3	144.0	2.3	-122.6	1.3	0.50	0.29	2.61	S_3
G6	-4.3	-2.0	78.6	2.9	-55.4	0.9	1.34	0.45	3.02	$S_J + B$
G7	-5.0	-2.0	82.6	3.0	-57.0	0.8	0.46	0.90	3.14	S_3
G8	-3.3	0.0	75.5	3.2	-49.9	1.6	1.34	0.50	3.57	S_3
G9	-3.6	-2.0	83.1	2.8	-59.4	1.0	0.67	0.47	2.99	$S_J + B$
G10	-2.6	-4.3	143.7	2.3	-119.5	1.1	0.65	0.23	2.51	S_3
G11	-4.2	-2.0	76.3	2.3	-58.5	0.8	0.81	0.70	2.41	S_3
G12	-3.4	-4.3	151.3	2.1	-122.1	1.1	0.25	0.22	2.37	G_b
G13	-3.0	-4.3	144.5	2.4	-125.4	0.9	0.28	0.18	2.60	G_b
G14	-2.8	-2.0	44.5	1.9	-21.2	1.1	0.30	0.31	2.18	G_b
G15	-2.8	-2.0	51.7	2.1	-32.1	0.9	0.42	0.29	2.31	S_3
G16	-2.7	-2.0	49.1	2.0	-27.5	1.1	0.73	0.40	2.26	S_3
G17	-4.3	-2.0	57.3	1.6	-40.9	0.7	0.45	0.36	1.72	S_3
G18	-3.7	0.0	44.5	1.7	-33.4	0.9	1.22	0.52	1.91	$S_J + B$

Table 1 Salient data for vDSSB predictions. ΔG_{vol} , standard state correction; ΔG_{fs} , finite size correction for charged guest molecule; $\langle W_{b/u} \rangle$, $\sigma_{b/u}$, AD_b, mean NE work, standard deviation and Anderson Darling test for the bound and unbound states; σ_{BU} , standard deviation of the convolution; Est. type, estimate type (see text). Energy unit is in kcal/mol.

normal). From the variance of the convolution σ_{BU}^2 , the bias can be readily estimated by a generating a sample of *normal distributions* with zero mean and variance σ_{BU}^2 and by computing the bias as

$$B(\sigma, n) = \left\langle \frac{1}{n} \sum^n e^{-\beta W} \right\rangle + \frac{1}{2} \sigma_{bu}^2 \quad (11)$$

where the exponential sum is averaged over all generated normal distributions. In Figure 3, we report the bias, Eq. 11 as a function of the number of points and of the variance. In our case, $n = 360 \times 480 = 182400$ while σ_{bu} varies in the range 2.3 (G4) up to 3.7 (G1), with a bias correction of the order of the fraction of kcal/mol in most cases and slightly higher than 1 kcal/mol only for G6, G7, G8 and G1.

In Table 2, we report in the second column the vDSSB submitted blind predictions (where the estimate was determined according to the previously cited criteria) along with the Gaussian estimate, the Gaussian mixture estimate (Eq. 7), and the bias-corrected Jarzynski estimate (not submitted). The uncertainties have been computed by bootstrapping with resampling the bound and unbound work samples *prior to* convolution, to avoid an artificial underestimation of the error when resampling from a boosted distribution[15]. In the last column, we report the electrostatic contribution (ΔG_q) to the overall dissociation free energy. In general, we can say that electrostatics is not the driving force for binding. In two cases, the electrostatic balance is unfavorable (G9, G18). For the small G7, most of the binding comes instead from electrostatics, very likely due to the presence of H-bonded water molecules at the

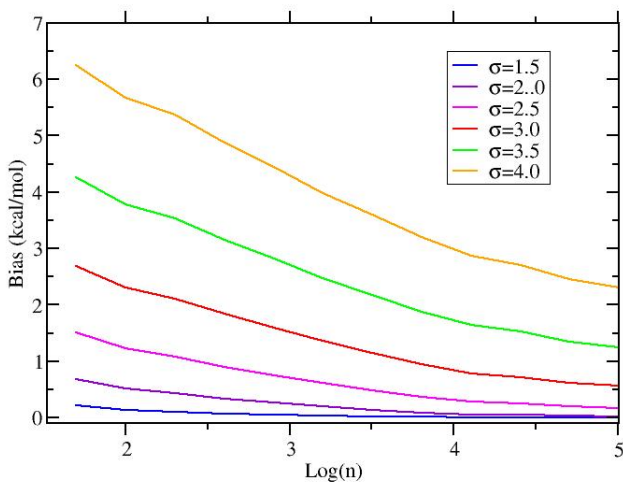


Fig. 3 Bias of the exponential average as a function of n and σ

entrance of the binding pocket as can be verified from the HREM trajectories provided on Zenodo (<https://zenodo.org/record/5891191>). The convergence of the prediction can be assessed by analyzing the vDSSB estimates, based on the above criteria, as a function of the duration time of the most dissipative process, i.e. the annihilation of the ligand in the bound state (see σ_u and σ_b entries in Table 1). From Figure 4, we can see that most of the predictions appear to have converged within the uncertainty, with only two exceptions (G2 and G5).

The correlation diagrams and metrics for all the estimates of Table 2 are reported in Figure 5 and Table 3. The large squares refer to the vDSSB ranked prediction. All predictions based on the estimates are strongly correlated one to the other, whether one chooses the sets including only thirteen guests from SAMPL9, the five additional ligands, and the set comprising all the eighteen ligands. Regarding the agreement with ITC data, we note that, while the Pearson's and Kendall correlation coefficients R_{xy} are acceptable (for the 13 SAMPL9 guests), good (for all the 18 systems) and excellent (for the 5 extra ligands), most of predictions appear to be systematically affected by a large *positive* bias [for the binding free energy (BFE)] of the order of 3 kcal/mol. Paraquat (G13) is a notable exception to this trend as the binding energy is in this case *underestimated* by less than 2 kcal/mol. However, this outcome could be due to a cancellation effect, with the prediction being actually much lower than the experimental counterpart when the former is corrected for the systematic and mean signed error.

This molecule was in fact included also in the SAMPL7 challenge for Isaac's TrimerTrip[5], and in our SAMPL7 submission paraquat was an outlier, with a strongly *underestimated* dissociation free energy, possibly due to the neglect

guest	Pred.	Exp.	Gauss	EM(3)	Jarz+bias	ΔG_q
G1	7.8± 0.6	-6.53	6.7 ± 1.1	8.5± 2.6	7.8± 0.6	-0.7 ± 1.2
G2	13.0± 1.2	-10.59	13.7 ± 0.8	13.0± 1.2	14.0± 0.6	1.0 ± 0.3
G3	11.0± 0.8	-8.03	8.2 ± 0.6	11.0± 0.8	11.1± 0.3	0.5 ± 0.8
G4	6.2± 0.8	-6.50	6.2 ± 0.4	7.3± 0.4	7.2± 0.4	1.2 ± 0.4
G5	7.2± 0.6	-5.46	6.8 ± 0.6	7.2± 0.6	7.4± 0.5	5.3 ± 0.2
G6	11.6± 0.4	-8.08	9.2 ± 1.2	11.9± 1.2	11.6± 0.4	0.3 ± 0.8
G7	11.5± 1.9	-7.07	10.3 ± 0.9	11.5± 1.9	12.3± 0.6	11.1 ± 0.7
G8	11.6± 1.6	-6.04	11.5 ± 1.1	11.6± 1.6	12.1± 0.8	2.1 ± 1.5
G9	11.8± 0.9	-6.32	10.4 ± 1.0	12.2± 1.9	11.8± 0.9	-0.5 ± 0.8
G10	12.7± 0.7	-9.96	12.0 ± 0.5	12.7± 0.7	13.0± 0.5	1.2 ± 0.3
G11	8.3± 0.5	-6.26	6.7 ± 0.4	8.3± 0.5	8.4± 0.4	0.7 ± 0.5
G12	16.8± 0.8	-11.02	16.8 ± 0.4	17.5± 0.3	17.6± 0.3	2.8 ± 0.2
G13	6.9± 1.0	-8.58	6.1 ± 0.8	6.9± 0.8	6.9± 0.5	1.5 ± 0.5
G14	14.5± 0.7	9.68	14.5 ± 0.7	15.0± 0.8	15.0± 0.6	5.2 ± 0.1
G15	10.7± 0.6	8.37	10.4 ± 0.5	10.7± 0.6	10.8± 0.6	4.9 ± 0.2
G16	12.9± 0.4	10.59	12.7 ± 0.6	12.9± 0.4	13.0± 0.3	5.1 ± 0.2
G17	8.0± 0.2	6.48	7.5 ± 0.3	8.0± 0.2	8.1± 0.2	2.5 ± 0.2
G18	4.9± 0.4	0.00	4.4 ± 0.5	4.9± 0.4	4.9± 0.4	-3.8 ± 0.3

Table 2 Estimates of the dissociation free energy in the vDSSB approach. Pred., submitted predictions; Exp., ITC data; Gauss, Gaussian estimates; EM(3), estimates based on Eq. 7; Jarz+bias, estimates based on Eq. 6; ΔG_q , estimated contribution of the electrostatic interactions to the binding (computed using the Gaussian assumption). Energy units are in kcal/mol.

Est.	R_{xy}	a	b	MUE	τ	MSE	npt
Pred	0.68	1.12	1.87	3.07	0.42	-2.77	13
Gauss	0.70	1.25	-0.10	2.29	0.29	-1.86	13
EM(3)	0.67	1.11	2.18	3.27	0.46	-3.01	13
Jar+B	0.69	1.19	1.66	3.39	0.38	-3.14	13
Pred	0.76	0.93	3.37	3.10	0.50	-2.88	18
Gauss	0.76	0.99	2.19	2.45	0.50	-2.14	18
EM(3)	0.77	0.95	3.49	3.27	0.54	-3.09	18
Jar+B	0.77	0.98	3.33	3.38	0.48	-3.19	18
Pred	0.93	0.84	4.27	3.18	0.80	-3.18	5
Gauss	0.92	0.88	3.70	2.88	0.80	-2.88	5
EM(3)	0.91	0.86	4.24	3.28	0.80	-3.28	5
Jar+B	0.92	0.87	4.25	3.34	0.80	-3.34	5

Table 3 Precision and accuracy metrics (see text) for the vDSSB estimates of Table 2.

of polarization in the bound state.^[31] To the light of the structural similarities of WP6 and the TrimerTrip, and as we used exactly the same force field for paraquat in both challenges, we would have expected G13 to be an outlier too in the SAMPL9 challenge. As a matter of fact, if we remove G13 (whose binding affinity was actually known before the submission), the Pearson correlation improves to 0.78 and the τ Kendall to 0.56 while the MUE becomes virtually identical to the MSE ($\simeq 3.1$ kcal/mol, see Table 5 further on).

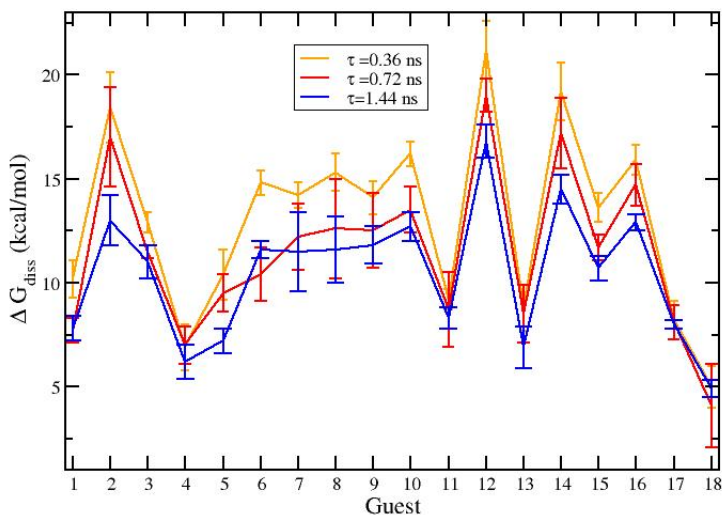


Fig. 4 Convergence of vDSSB estimates of the dissociation free energy as a function of the duration time of the bound state NE alchemical transitions for the eighteen guest molecules reported in Figure 1.

4 Discussion

In Table 4 we succinctly describe the five ranked submissions to the SAMPL9 challenge. The Serrilon submission was done using machine learning methods

Sub.	Method	FF	Restr.	Charge corr.	Neutr.
Voelz	ALCH	OpenFF2.0/AM1BCC	COM(strong)	?	12 Na+
vDSSB	ALCH	GAFF2/AM1BCC	COM (weak)	PME	UBP
Ponder	ALCH	AMOEBA	COM	PME	12 Na+
He	PB/SA	GAFF2/ABCG2	n/a	?	12 Na+/PB
Serrilon	ML	n/a	n/a	n/a	n/a

Table 4 Methodological information on the SAMPL9 ranked submissions. ALCH, alchemical; ML, Machine Learning; PB/SA, Poisson Boltzmann, implicit solvent; FF, force field; Restr., host-guest restraint type; Charge corr., correction for charged ligands (finite size); Neutr., Neutralization procedure for the bound state; UB, uniform background plasma.

based on a neural network. The He prediction was based on an MM-PB/SA approach (implicit solvent) on conformations generated by molecular dynamics with explicit solvent using the GAFF2 force field. We then count three MD-based submissions, using a common alchemical approach each with a different force field, namely the fixed-charge GAFF2/AM1-BCC[35] (vDSSB,

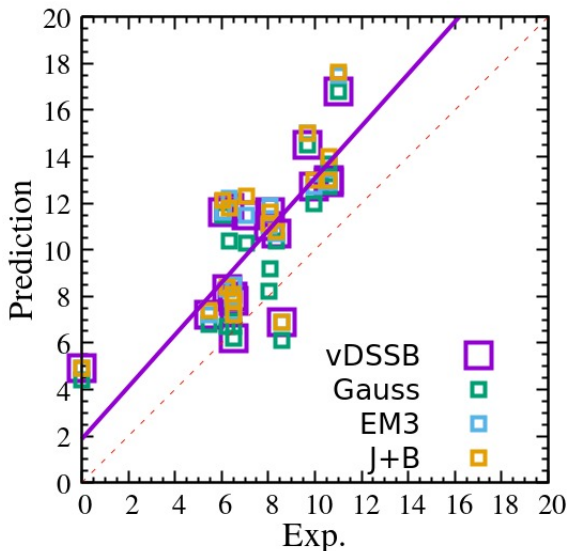


Fig. 5 Correlation diagram for vDSSB-based dissociation free energy estimates reported in Table 2

the present submission), OpenFF2.0[46] (Voltz) and the polarizable force field AMOEBA[47] (Ponder). The Ponder and Voelz calculations were done using the traditional free energy perturbation approach with equilibrium simulations for each intermediate alchemical state along the λ -stratification. No enhanced sampling was used in Ponder while in Voelz λ -hopping enforced via a serial generalized ensemble (SGE) approach[48–50] with adaptive weights was used (termed “Expanded Ensemble”). In λ -hopping, states can exchange λ values so that an SGE trajectory can visit all λ intermediate states. However, no scaling of the potential energy barriers is enforced, as in e.g. FEP+[51] or in the end-states of vDSSB.[15] The effectiveness of λ -exchanges via HREM was recently assessed in Ref. [52] where “HREX enhancement [did] not appear to give a significant boost to the FEP accuracy”.

At variance with vDSSB where a uniform neutralizing background was adopted, the MD-based Voelz and Ponder used 12 Na^+ counterions in the bound state. In Table 5, we report results of the ranked submissions for the SAMPL9 challenge using as metrics the Pearson correlation coefficient R_{xy} , the slope a and intercept b of the best fitting line, the Kendall ranking coefficient τ , and the mean unsigned and signed errors MUE, MSE. As far as correlation is concerned, the three MD-alchemy submissions perform decently, with the Ponder set featuring the best prediction for both R_{xy} and τ and with vDSSB yielding the best fitting line. Ponder is still the best correlated prediction ($R_{xy} = 0.90$) if the G13 guest, with known BFE at the time of

Submission	R_{xy}	a	b	τ	MUE	MSE
Serillon	0.38	0.36	-5.58	0.18	1.56	0.61
He	0.63	0.65	-4.61	0.53	1.89	1.87
Ponder	0.76	1.58	5.28	0.59	1.98	-0.79
Voeltz	0.72	1.51	3.25	0.51	2.27	0.68
vDSSB	0.68	1.12	-1.87	0.42	3.07	2.77
Serillon ^a	0.35	0.32	-5.73	0.06	1.56	0.53
He ^a	0.63	0.64	-4.62	0.48	1.92	1.90
Ponder ^a	0.90	1.42	4.61	0.61	1.58	-1.42
Voeltz ^a	0.73	1.53	3.35	0.58	2.45	0.73
vDSSB ^a	0.78	1.22	-1.44	0.56	3.19	3.14

^a Metrics computed by eliminating G13 (see text).

Table 5 Results for the SAMPL9 ranked submissions; Metrics has been. MUE, MSE, and b are given in kcal/mol.

the challenge, is removed from the set. The AMOEBA polarizable force field used in the Ponder submission already performed quite well in the SAMPL7 challenge on the Isaac’s TrimerTrip[5], hence confirming the importance of charge reorganization/polarization in highly polar or charged molecules such as CBN-like compounds or WP6. While the MUE is in the range of 2:3 kcal/mol for Ponder, Voeltz and vDSSB, the MSE is positive and large *only* for our prediction, with the majority of the dissociation free energies significantly overestimated. This fact can also be visually appreciated from Figure 6, where the correlation diagrams for the five ranked submissions are reported. Incidentally, we note that the BFE of G13/paraquat (red highlighted symbols) in Serillon (-8.68 kcal/mol), Voeltz and He (10.2 kcal/mol) is in accord either with the experimental value using fluorimetric assay reported in Ref. [7] or with the ITC-determined association constant provided in Ref. [8]. A systematic overestimation of our vDSSB dissociation free energies was expected, since, before the submission deadline, we found excellent correlation for the five compounds G14-G18 with known ΔG_d^0 but we also found a significant mean MSE (see Table 3). In the original submission text file[53] we in fact wrote: ”given the negative [for dissociation free energy] MSE found in the pre-assessment, we expect a consistent overestimation (in the order of 2-3 kcal/mol) of the submitted BFE, possibly due the presence of protonated WP6 species at ph=7.4”. However, such striking discrepancy cannot be attributed to the systematic contribution of complexes with WP6 in different protonation states as the experimentally determined weight of the WP6⁻¹² species at pH=7.4 is found to be close to unity. Besides, the large MSE is not observed in the other two alchemy-based predictions. The large MSE in our case is probably caused by the approach used in the neutralization of the MD box in the bound state. Both in Voeltz and Ponder MD-based submissions, neutralization of the 12 negative charges of the host was achieved by introducing an equivalent number of Na⁺ counterions. In our prediction, no counterions were used and neutralization was imposed naturally by the PME approach by way a uniform background plasma with constant charge density $\rho = 12/V_{\text{box}}$, using the finite size correction (Eq. 9) for charged guests on the computed ΔG_d^0 . By analyzing the

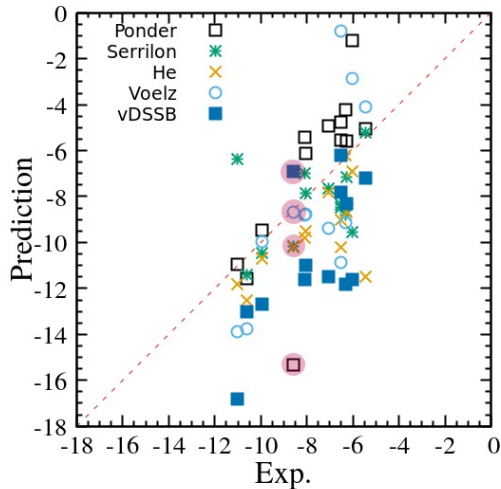


Fig. 6 Correlation diagrams of experimental and calculated binding free energy (units of kcal/mol) for the five ranked submissions. The red-highlighted symbols refers to G13 (paraquat).

HREM trajectories of the bound state, we found that the WP6 toroidal cavity allocating the guest molecule in most of the cases remains completely devoid of water molecules, hence exhibiting a lower mean dielectric constant than that of the surrounding bulk. In Ref. [54], Hub *et al.* showed that, when using a uniform background neutralizing distribution in the context of PBC/PME, artifacts may arise in particular in systems with an inhomogeneous dielectric constant. More in detail, the authors demonstrated that the background charge artificially cause the charged guest to *favor the lower dielectric environment*. The authors provided a simplified correction, based on the Poisson-Boltzmann model, for the free energy difference in the two dielectrics (bulk water and low dielectric environment). For spherical geometry, the correction reads

$$\Delta V = -2\pi \frac{q_{\text{guest}} \rho_{\text{BG}} r_0^2}{\epsilon_l} \quad (12)$$

where ϵ_l is the permittivity of the low-dielectric, r_0 is the radius of the sphere, and ρ_{BG} is the uniform background charge density. The approximated correction Eq. 12 for the spherical geometry cannot be lightly used for the WP6 toroidal cavity with an unknown permittivity, possibly dependent on the guest size and topology. However, we can use Eq. 12 to have an order of magnitude of this correction. If we set ϵ_l in the range 2:4, and $r_0 = 3.5 : 4 \text{ \AA}$ (the effective radius of the WP6 cavity), we find corrections in the range -1.8:3.0 kcal/mol. For the Voelz and Ponder prediction sets these corrections are one order of

magnitude smaller as their ρ_{BG} includes *only* the neutralizing charge for the guest molecule being the WP6⁻¹² anion neutralized by the twelve Na⁺ cations.

A Hub-like correction for inhomogeneous dielectric environments in the WP6 complexation may indeed explain why our dissociation free energies, obtained with a neutralizing uniform ρ of 12 positive charges, are systematically overestimated while in Voelz and Ponder submissions, where the neutralization was achieved by adding twelve explicit cations, positive and negative MSE below 1 kcal/mol were found. Moreover, the correction Eq. 12 would make the dicationic G13 guest an outlier with an MSE in the range -4:-5 kcal/mol. If we eliminate G13 from the set, such outcome is consistent with the result obtained for G13 in the case of the SAMPL7 TrimerTrip (characterized by a quasi-toroidal cavity of similar size as WP6) where the dissociation free energy was underestimated by more than 5 kcal/mol using the same force field and a strictly related MD-based alchemical approach.[31] On the other hand, it should be noted that the vDSSB dissociation free energy of the *chiral* dicationic G12 guest even corrected using Eq. 12, would still be significantly overestimated. In this case, a possible explanation for the discrepancy can be that, as the experimental binding constant refers to the *racemic* mixture[6], the affinities of the two bulky stereoisomers are disparate and the effective binding constant would be dominated by the *weakest* binder.

Verifying the hypothesis for the consistent overestimation of the dissociation free energy stemming from the uniform background plasma is straightforward but costly. We would need to repeat all HREM and NE calculations for the bound state resizing our MD box using a sidelength of $\simeq 60$ Å to match the experimental Na⁺ concentration of 0.14 M[6], increasing the volume (and the cost) by a factor of four. Besides, convergence of a solution containing diffusing cations and a single heavily charged host-guest complex is certainly harder than that where neutralization is provided by a constant uniform background. In vDSSB, canonical sampling is essential in the end-state for the bound complex. Our HREM scaling protocol, as stated in the Methods section, only involves intra-solute interactions leaving unaltered the solute-solvent balance so as not to accelerate passive diffusion. This is certainly an asset in our approach as the impact on the residence time of the (weakly restrained) guest in the binding pocket is limited but can be an important shortcoming when using explicit counterions by significantly slowing down convergence.

5 Potential pitfalls and weak points in vDSSB

We have previously seen that the estimate type from the work convolution for ΔG_{vdssb} is based on Eq. 6, 7 or on the Gaussian assumption depending on the character of the bound and unbound work distributions as assessed by the AD test or on the uncertainty of the EM estimate. Eq. 6 is used when the AD tests fail and when the EM estimate on the convolution has a large (≥ 2.0 kcal/mol) uncertainty. In this case Eq. 6 is corrected for a theoretical σ and n dependent positive bias computed from a Gaussian distribution with

the same variance of the convolution work distribution. If the latter departs significantly from a normal distribution, the bias can be overestimated with an impact on the accuracy of ΔG_{vdssb} .

A weak point of *any* alchemical approach, including vDSSB, is related to the standard state correction, connected to the elusive binding site volume[31, 55–57]. In vDSSB, where a weak COM-COM restraint is used, the *negative* correction to the *dissociation* free energy is estimated from the variance of the host-guest COM-COM distance distribution in the bound state and is hence a characteristic of the host-guest complex, varying in a range -5:-2.5 kcal/mol (see Table 1). In principle, the binding site volume should depend on both the host and the guest in the context of the NE alchemical theory[29]. In Voelz and Ponder FEP calculations, the volume correction is related to the force constant of the host-guest COM-COM restraint as $V_{\text{restr}} = (\frac{2\pi RT}{k})^{3/2}$ and, as such, is *identical for all guests*, in the assumption that in the simulation of the restrained complex all states that are made accessible by restrained potential have been canonically sampled for all λ states along the alchemical path[55, 57]. Such correction to the dissociation free energy is equal to -3.85 in Voelz[58]. In Ponder, again an *identical* volume correction was used for all guests using COM-COM restraints defining a flat-bottom potential “chosen such that [these restraints] were not violated during unrestrained simulations runs on the bound host-guest complex.”[59] The size of the Ponder standard state correction was not given in Ref. [59]. If we remove our guest-dependent standard state volume correction (ΔG_{vol} entry in Table 1) assuming an identical correction of -4 kcal/mol for all guests as in Ponder and Voelz, agreement with experiment luckily improves, yielding $R_{xy} = 0.84$, $\tau = 0.49$, $a = 1.60$, MUE=2.18 kcal/mol and MSE=1.50.

6 Conclusion

We have presented our results on the SAMPL9 challenge focusing on binding of soluble carboxy-pillar[6]arene)with ammonium/diammonium cationic guests. We adopted an alchemical technique, named virtual double system single box, relying on an enhanced sampling of the end-states and on the production of few hundreds of fast nonequilibrium trajectories where the ligand is decoupled and recoupled in the bound and unbound state, respectively. The resulting work distributions were combined (convoluted) as if the two independent processes occurred in the same box, with one ligand on the host and the other in the far distant bulk. The dissociation free energy was estimated from the convolution using the Jarzynski theorem, the Gaussian assumption, or the Gaussian mixture assumption, depending on the character of the bound and unbound work distributions.

Correlation with experimental data is acceptable and consistent with our previous SAMPL6 and SAMPL7 submission also based on nonequilibrium alchemy. If G13 (paraquat), whose experimental binding constant was known at the time of the challenge[53], is removed from the set, vDSSB is the second

best-correlated submission of the challenge (see Table 5). Nonetheless, when compared to the other two MD-based SAMPL9 alchemical submissions, our prediction set for the dissociation free energy exhibits a large mean signed error (MSE), suggesting a systematic error in the simulation protocol. We attribute the large MSE to the way neutralization was imposed in the bound state containing the WP6⁻¹² anion and the guest. At variance with the other MD-based submissions, where explicit counterions were introduced, we used a uniform neutralizing background plasma. The uniform background charge approach has been recently demonstrated to artificially favor the binding in the lower dielectric environment.

Overall, the challenge has confirmed that MD-based alchemical methods tend to correlate better with experiment with respect to other approaches (e.g. Machine Learning or Poisson-Boltzmann with MD sampling of the end-states). However, accuracy is still falling short in MD protocols, with a mean deviation of the order of 2 kcal/mol even when resorting to computationally demanding polarizable force field. In this regard, we note that the present SAMPL9 challenge (as well as some of the past challenges) is characterized by exceptionally critical issues from the parameterization perspective mostly related to electrostatic interactions, such as unknown protonation state of the highly charged host molecule, chiral specificity in binding, singly or doubly charged guests. Besides, in most of the recent SAMPL initiatives, all guest molecules share in general a common chemical structure, characterized by charged substituents on a hydrophobic scaffold while the hosts are rigid macrocyclic molecules heavily decorated with polar or charged groups. As recently shown in Ref. [60], small imperfections on the electrostatic modeling can have a huge impact on the BFE. Possibly, these imperfections could be systematically enhanced when testing MD-based approaches with “general” electrostatic parameterizations in the recent SAMPL challenges.

Supplementary information. The bound and unbound state work distributions for all eighteen ligands of Figure 1 are reported in the Supporting Information. PDB trajectory files, raw work data, and force field parameter files are available at the general-purpose open-access repository Zenodo (<https://zenodo.org/record/5891191>).

The ORAC program (v6.1) is available for download under the GPL at the website <http://www1.chim.unifi.it/orac/>

Third-party software Autodock Vina can be downloaded from the website <https://vina.scripps.edu/>

Acknowledgments. The computing resources and the related technical support used for this work have been provided by CRESCO/ENEAGRID High Performance Computing infrastructure and its staff. CRESCO/ENEAGRID m, High Performance Computing infrastructure is funded by ENEA, the Italian National Agency for New Technologies, Energy and Sustainable Economic Development and by Italian and European research programmes (see www.cresco.enea.it for information).

References

- [1] Hari S. Muddana, Andrew T. Fenley, David L. Mobley, and Michael K. Gilson. The sampl4 host–guest blind prediction challenge: an overview. *J. Comput Aided Mol. Des.*, 28(4):305–317, 2014.
- [2] Jian Yin, Niel M. Henriksen, David R. Slochower, Michael R. Shirts, Michael W. Chiu, David L. Mobley, and Michael K. Gilson. Overview of the sampl5 host–guest challenge: Are we doing better? *J. of Comput. Aided Mol. Des.*, pages 1–19, 2016.
- [3] Andrea Rizzi, Steven Murkli, John N. McNeill, Wei Yao, Matthew Sullivan, Michael K. Gilson, Michael W. Chiu, Lyle Isaacs, Bruce C. Gibb, David L. Mobley, and John D. Chodera. Overview of the sampl6 host–guest binding affinity prediction challenge. *J. Comput. Aided Mol. Des.*, 32(10):937–963, Oct 2018.
- [4] Andrea Rizzi, Travis Jensen, David R. Slochower, Matteo Aldeghi, Vytautas Gapsys, Dimitris Ntekoumes, Stefano Bosisio, Michail Papadourakis, Niel M. Henriksen, Bert L. de Groot, Zoe Cournia, Alex Dickson, Julien Michel, Michael K. Gilson, Michael R. Shirts, David L. Mobley, and John D. Chodera. The sampl6 sampling challenge: Assessing the reliability and efficiency of binding free energy calculations. *bioRxiv*, 2019. DOI: 10.1101/795005.
- [5] M. Amezcua, L. El Khoury, and D. L. Mobley. Sampl7 host-guest challenge overview: assessing the reliability of polarizable and non-polarizable methods for binding free energy calculations. *J. Comput.-Aided Mol. Des.*, 35(1):1–35, 2021.
- [6] Chun-Lin Deng, Ming Cheng, Peter Y. Zavalij, and Lyle Isaacs. Thermodynamics of pillararene guest complexation: blinded dataset for the sampl9 challenge. *New J. Chem.*, 46:995–1002, 2022.
- [7] Guocan Yu, Xiangyan Zhou, Zibin Zhang, Chengyou Han, Zhengwei Mao, Changyou Gao, and Feihe Huang. Pillar[6]arene/paraquat molecular recognition in water: High binding strength, ph-responsiveness, and application in controllable self-assembly, controlled release, and treatment of paraquat poisoning. *J. Am. Chem. Soc.*, 134(47):19489–19497, 2012.
- [8] Henning Nicolas, Bin Yuan, Jiangfei Xu, Xi Zhang, and Monika Schönhoff. ph-responsive host-guest complexation in pillar[6]arene-containing polyelectrolyte multilayer films. *Polymers*, 9(12), 2017.
- [9] <https://github.com/samplchallenges/SAMPL8>, accessed 13 January 2022.

- [10] Kui Yang, Jia Wen, Shuang Chao, Jing Liu, Ke Yang, Yuxin Pei, and Zhichao Pei. A supramolecular photosensitizer system based on the host-guest complexation between water-soluble pillar[6]arene and methylene blue for durable photodynamic therapy. *Chem. Commun.*, 54:5911–5914, 2018.
- [11] Dóra Hessz, Stella Bádogos, Marton Bojtar, Istvan Bitter, Laszla Drahos, and Miklos Kubinyi. Complexes of carboxylato pillar[6]arene with brooker-type merocyanines: Spectral properties, pka shifts and the design of a displacement assay for trimethyl lysine. *Spectrochimica Acta Part A: Molecular and Biomolecular Spectroscopy*, 252:119455, 2021.
- [12] Bin Hua, Li Shao, Zhihua Zhang, Jifu Sun, and Jie Yang. Pillar[6]arene/acridine orange host-guest complexes as colorimetric and fluorescence sensors for choline compounds and further application in monitoring enzymatic reactions. *Sensors and Actuators B: Chemical*, 255:1430–1435, 2018.
- [13] F. Iannone, F. Ambrosino, G. Bracco, M. De Rosa, A. Funel, G. Guarnieri, S. Migliori, F. Palombi, G. Ponti, G. Santomauro, and P. Procacci. Cresco enea hpc clusters: a working example of a multifabric gpus spectrum scale layout. In *2019 International Conference on High Performance Computing Simulation (HPCS)*, pages 1051–1052, 2019.
- [14] Piero Procacci, Marina Macchiagodena, Marco Pagliai, Guido Guarnieri, and Francesco Iannone. Interaction of hydroxychloroquine with sars-cov2 functional proteins using all-atoms non-equilibrium alchemical simulations. *Chem. Commun.*, 56:8854–8856, 2020.
- [15] Marina Macchiagodena, Marco Pagliai, Maurice Karrenbrock, Guido Guarnieri, Francesco Iannone, and Piero Procacci. Virtual double-system single-box: A nonequilibrium alchemical technique for absolute binding free energy calculations: Application to ligands of the sars-cov-2 main protease. *J. Chem. Theory Comput.*, 16(11):7160–7172, 2020.
- [16] Macchiagodena Marina, Karrenbrock Maurice, Pagliai Marco, Guarnieri Guido, Iannone Francesco, and Procacci Piero. *Nonequilibrium Alchemical Simulations for the Development of Drugs Against Covid-19*, pages 1–41. Springer Nature, New York, NY., 2021.
- [17] Marina Macchiagodena, Maurice Karrenbrock, Marco Pagliai, and Piero Procacci. Virtual double-system single-box for absolute dissociation free energy calculations in gromacs. *J. Chem. Inf. Model.*, 61(11):5320–5326, 2021.
- [18] Y. Sugita and Y. Okamoto. Replica-exchange molecular dynamics method for protein folding. *Chem. Phys. Lett.*, 314:141–151, 1999.

- [19] SciFinder; Chemical Abstracts Service: Columbus, OH; carbon-13 NMR spectrum; spectrum ID CC-03-C_SPC-3734; RN 50-52-2; <https://scifinder.cas.org> (accessed January 13, 2022).
- [20] D.D. Perrin, B. Dempsey, and E.P. Serjeant. *pKa Prediction for Organic Acids and Bases*, chapter Molecular Factors that Modify pKa Values. Springer, 1981.
- [21] Sampl9: Experimental results. <https://github.com/samplchallenges/SAMPL9/tree/main/experimental> accessed 13 January 2022.
- [22] S. Marsili, G. F. Signorini, R. Chelli, M. Marchi, and P. Procacci. Orac: A molecular dynamics simulation program to explore free energy surfaces in biomolecular systems at the atomistic level. *J. Comput. Chem.*, 31:1106–1116, 2010.
- [23] C. Jarzynski. Nonequilibrium equality for free energy differences. *Phys. Rev. Lett.*, 78:2690–2693, 1997.
- [24] G. E. Crooks. Nonequilibrium measurements of free energy differences for microscopically reversible markovian systems. *J. Stat. Phys.*, 90:1481–1487, 1998.
- [25] Piero Procacci. Unbiased free energy estimates in fast nonequilibrium transformations using gaussian mixtures. *J. Chem. Phys.*, 142(15):154117, 2015.
- [26] An EM Fortran90 code is available with the ORAC6 distribution tarball at the ORAC site www.chim.unifi.it/orac .
- [27] Jeff Bilmes. A gentle tutorial of the em algorithm and its application to parameter estimation for gaussian mixture and hidden markov models. Technical report, International Computer Science Institute, Berkeley, CA, 1998.
- [28] T. W. Anderson and D. A. Darling. A test of goodness of fit. *J. Am. Stat. Ass.*, 49:765–769, 1954.
- [29] Piero Procacci. I. dissociation free energies of drug-receptor systems via non-equilibrium alchemical simulations: a theoretical framework. *Phys. Chem. Chem. Phys.*, 18:14991–15004, 2016.
- [30] Piero Procacci, Massimiliano Guarrasi, and Guido Guarnieri. Sampl6 host-guest blind predictions using a non equilibrium alchemical approach. *J. Comput.-Aided Mol. Des.*, 32:965–982, 2018.

- [31] Piero Procacci and Guido Guarnieri. Sampl7 blind predictions using nonequilibrium alchemical approaches. *J. Comput.-Aided Mol. Des.*, 35(1):37–47, 2021.
- [32] Tom Darden, David Pearlman, and Lee G. Pedersen. Ionic charging free energies: Spherical versus periodic boundary conditions. *J. Chem. Phys.*, 109(24):10921–10935, 1998.
- [33] Piero Procacci. Myeloid cell leukemia 1 inhibition: An in silico study using non-equilibrium fast double annihilation technology. *J. Chem. Theory Comput.*, 14(7):3890–3902, 2018.
- [34] Piero Procacci. Primadorac: A free web interface for the assignment of partial charges, chemical topology, and bonded parameters in organic or drug molecules. *J. Chem. Inf. Model.*, 57(6):1240–1245, 2017.
- [35] GAFF and GAFF2 are public domain force fields and are part of the AmberTools distribution, available for download at <https://amber.org> internet address (accessed January, 2022). According to the AMBER development team, the improved version of GAFF, GAFF2, is an ongoing project aimed at "reproducing both the high quality interaction energies and key liquid properties such as density, heat of vaporization and hydration free energy". GAFF2 is expected "to be an even more successful general purpose force field and that GAFF2-based scoring functions will significantly improve the successful rate of virtual screenings."
- [36] Xue Dong, Xinghang Yuan, Zhenlei Song, and Qiantao Wang. The development of an amber-compatible organosilane force field for drug-like small molecules. *Phys. Chem. Chem. Phys.*, 23:12582–12591, 2021.
- [37] Arthur J. Trott, Oleg nd Olson. Autodock vina: Improving the speed and accuracy of docking with a new scoring function, efficient optimization, and multithreading. *J. Comput. Chem.*, 31(2):455–461, 2010.
- [38] S. Izadi and A. V. Onufriev. Accuracy limit of rigid 3-point water models. *J. Chem. Phys.*, 145(7):074501, 2016.
- [39] U. Essmann, L. Perera, M. L. Berkowitz, T. Darden, H. Lee, and L. G. Pedersen. A smooth particle mesh ewald method. *J. Chem. Phys.*, 103:8577–8593, 1995.
- [40] M. Parrinello and A. Rahman. Crystal structure and pair potentials: A molecular-dynamics study. *Phys. Rev. Lett.*, 45:1196–1199, Oct 1980.
- [41] Shuichi Nosé. A unified formulation of the constant temperature molecular dynamics methods. *J. Chem. Phys.*, 81(1):511–519, 1984.

- [42] Piero Procacci. Hybrid MPI/OpenMP Implementation of the ORAC Molecular Dynamics Program for Generalized Ensemble and Fast Switching Alchemical Simulations. *J. Chem. Inf. Model.*, 56(6):1117–1121, 2016.
- [43] Lorentz Jäntschi and Sorana D. Bolboaca. Computation of probability associated with anderson-darling statistic. *Mathematics*, 6(6):88, 2018.
- [44] Jeff Gore, Felix Ritort, and Carlos Bustamante. Bias and error in estimates of equilibrium free-energy differences from nonequilibrium measurements. *Proc. Natnl. Acad. Sci.*, 100(22):12564–12569, 2003.
- [45] Piero Procacci and Marina Macchiagodena. On the ns-dssb unidirectional estimates in the sampl6 sampling challenge. *J. Comput.-Aided Mol. Des.*, 35(10):1055–1065, 2021.
- [46] Open force field, an open and collaborative approach to better force field. <https://openforcefield.org/> accessed 13 January 2022.
- [47] Changsheng Zhang, Chao Lu, Zhifeng Jing, Chuanjie Wu, Jean-Philip Piquemal, Jay W. Ponder, and Pengyu Ren. Amoeba polarizable atomic multipole force field for nucleic acids. *J. Chem. Theory Comput.*, 14(4):2084–2108, 2018.
- [48] B.A. Berg and T. Neuhaus. Multicanonical Algorithms for 1st order phase-transitions. *Phys. Letters B*, 267(2):249–253, 1991.
- [49] R. Chelli. Optimal weights in serial generalized-ensemble simulations. *J. Chem. Theory Comput.*, 6:1935–1950, 2010.
- [50] Fugao Wang and D. P. Landau. Efficient, multiple-range random walk algorithm to calculate the density of states. *Phys. Rev. Lett.*, 86:2050–2053, 2001.
- [51] Lingle Wang, Yujie Wu, Yuqing Deng, Byungchan Kim, Levi Pierce, Goran Krilov, Dmitry Lupyan, Shaughnessy Robinson, Markus K. Dahlgren, Jeremy Greenwood, Donna L. Romero, Craig Masse, Jennifer L. Knight, Thomas Steinbrecher, Thijs Beuming, Wolfgang Damm, Ed Harder, Woody Sherman, Mark Brewer, Ron Wester, Mark Murcko, Leah Frye, Ramy Farid, Teng Lin, David L. Mobley, William L. Jorgensen, Bruce J. Berne, Richard A. Friesner, and Robert Abel. Accurate and reliable prediction of relative ligand binding potency in prospective drug discovery by way of a modern free-energy calculation protocol and force field. *J. Am. Chem. Soc.*, 137(7):2695–2703, 2015.
- [52] Vytautas Gapsys, Ahmet Yildirim, Matteo Aldeghi, Yuriy Khalak, David van der Spoel, and Bert L. de Groot. Accurate absolute free energies

- for ligand-protein binding based on non-equilibrium approaches. *Comm. Chem.*, 4(1):61, 2021.
- [53] WP6_vDSSB.txt: Original submission txt file in the /Analysis/Submissions directory. https://github.com/samplchallenges/SAMPL9/blob/main/host_guest/ accessed 13 January 2022.
- [54] Jochen S. Hub, Bert L. de Groot, Helmut Grubmüller, and Gerrit Groenhof. Quantifying artifacts in ewald simulations of inhomogeneous systems with a net charge. *J. Chem. Theory Comput.*, 10(1):381–390, 2014. PMID: 26579917.
- [55] Piero Procacci and Riccardo Chelli. Statistical Mechanics of Ligand-Receptor Noncovalent Association, Revisited: Binding Site and Standard State Volumes in Modern Alchemical Theories. *J. Chem. Theory Comput.*, 13(5):1924–1933, 2017.
- [56] Hengbin Luo and Kim Sharp. On the calculation of absolute macromolecular binding free energies. *Proc. Natnl. Acad. Sci. USA*, 99(16):10399–10404, 2002.
- [57] M. K. Gilson, J. A. Given, B. L. Bush, and J. A. McCammon. The statistical-thermodynamic basis for computation of binding affinities: A critical review. *Biophys. J.*, 72:1047–1069, 1997.
- [58] WP6-voelz-lab_EE_ranked.txt: Original submission txt file with Voelz predictions. https://github.com/samplchallenges/SAMPL9/blob/main/host_guest/ accessed 13 January 2022.
- [59] WP6-ponder.txt: Original submission txt file with Ponder predictions. https://github.com/samplchallenges/SAMPL9/blob/main/host_guest/ accessed 13 January 2022.
- [60] Dario Vassetz, Marco Pagliai, and Piero Procacci. Assessment of gaff2 and opls-aa general force fields in combination with the water models tip3p, spce, and opc3 for the solvation free energy of druglike organic molecules. *J. Chem. Theory Comput.*, 15(3):1983–1995, 2019.